

1 **Mn- Fe systematics in major planetary body reservoirs in the Solar System and the**
2 **positioning of the Angrite Parent body: A crystal chemical perspective**

3 **James J. Papike¹, Paul V. Burger¹, Aaron S. Bell¹, and Charles K. Shearer¹**

4 ¹Institute of Meteoritics, Department of Earth and Planetary Sciences,
5 University of New Mexico, Albuquerque, New Mexico 87131, U.S.A

6 **Submitted to American Mineralogist as a “Letter”**

7
8
9 **ABSTRACT**

10 A revised diagram plotting the Fe/ Mn ratio of pyroxene and olivine verses the anorthite
11 content of plagioclase indicates that the angrite parent body originated from a solar system
12 reservoir with a similar Mn-Fe signature to that from which the Earth was derived. The major
13 difference in terrestrial and angritic basalts is the extreme volatile depletion (particularly Na and
14 K) in the latter.

15 Considerable research and publication has been focused on angrite meteorites which are
16 among the oldest objects in the solar system (~4.56 Ga; Keil 2012). These meteorites include a
17 silica-undersaturated mafic mineral assemblage. The identity and location of their parent body is
18 still unknown and widely debated. Our new work on angrites SAH 99555, LEW 86010, NWA
19 10463, LEW 87051, and Angra dos Reis focused on olivine and is interpreted in the context of
20 existing pyroxene and plagioclase datasets. This paper improves the “Mn-Fe in olivine and
21 anorthite content of plagioclase tool for planetary parentage” specifically targeted at finding
22 members of the angrite group of meteorites.

24

INTRODUCTION

25

26

27

28

29

30

31

32

33

34

35

36

37

38

39

40

41

42

43

44

45

46

In a previous study (Papike et al. 2003), we presented a simple technique using the electron microprobe to determine planetary parentage of basaltic meteorites. This tool is based on Mn-Fe systematics in olivine and pyroxene and the anorthite content of plagioclase. This technique was specific to basalts, and was only to be applied to non-thermally annealed phases (pyroxene, olivine, and plagioclase lacking exsolution). Angrite melts are truly basalts according to the definition adopted by The Basaltic Volcanism in the Solar System Project (BVSP; 1981), the definition we will adhere to in this manuscript. Basalts are melts or near melts with <52% SiO₂, >6% CaO and Al₂O₃, and <12% MgO. Pyroxene, plagioclase, and olivine are the major phases. This technique has been used by many researchers as a quick and easy method to determine planetary parentage best used alongside other metrics of planetary parentage like oxygen isotopes. In a summary diagram in Papike et al. (2003; Fig. 4) based on the Fe/Mn ratio of olivine and pyroxene (y-axis) and anorthite content of plagioclase (x-axis), the position of the angrite parent body was plotted in the wrong location. At that time, only angrite pyroxene was plotted on the diagram. The first author did not realize that angrite pyroxene was not effective on this diagram because the M2 crystallographic site (a 6- to 8-fold coordinated, highly compliant site) was filled with Ca due to the high Ca concentration of the melt. Both the pyroxene M2 site and M1 site (octahedral) must be in play for pyroxene to be used to determine the correct Fe/Mn ratio. If the M2 site is completely filled with Ca, Mn partitioning in pyroxene is severely limited. In this paper we avoid these complications; we present a simple method to identify meteorite members of the angrite suite using the Fe/Mn ratio in angrite olivine and add constraints to the location of the angrite parent body (APB).

ANALYTICAL APPROACH

47 Thin sections of Sahara 99555, LEW 86010, NWA 10463, LEW 87051 and Angra dos
48 Reis were examined and documented using back-scattered electron (BSE) imaging on the JEOL
49 JXA-8200 electron microprobe (EMP) in the Institute of Meteoritics. Wavelength dispersive X-
50 ray maps were collected for Ca, Mn, and Cr, while energy dispersive (EDS) maps were collected
51 for Mg (note Figure 1). Quantitative point analyses of angrite olivine were conducted at an
52 accelerating voltage of 15 kV, a beam current of 10 nA, and a spot size from 1-3 μm . Elements
53 were standardized using a combination of Taylor Corp. Electron Microprobe mineral standards
54 as well mineral standards that have been developed in-house. Individual olivine microprobe
55 analyses are presented in an electronic appendix. In those figures where the Fe/Mn ratio is used
56 to distinguish planetary bodies (Figs. 3 and 5), only those olivine analyses with <5 mol.% Ca
57 endmember were used. While we acknowledge that this cutoff is somewhat arbitrary, one can
58 readily observe from the olivine quadrilaterals (Fig. 4), that over this range, the relationship
59 between Fe, Mg, and Ca is most linear, and is most likely to represent an igneous fractionation
60 trend, and is therefore the most relevant in the determination of a planetary parentage slope.

61

62

RESULTS

63 The results of the EMP analysis are illustrated in five figures. Figure 1 includes BSE, Mg,
64 Ca, Mn, and Cr maps of SAH 99555, NWA 10463, and LEW 86010. This order also represents
65 the cooling sequence, from fastest to slowest. SAH 99555 represents a near melt composition
66 and shows primary magmatic growth zoning which enables the ^{53}Mn - ^{53}Cr chronometer (Papike
67 et al. 2016a). Next is NWA 10463 which has exsolution only in the Fe-enriched rims. Next is
68 LEW 86010, with well developed exsolution in two directions throughout the olivine grains.
69 Last in the sequence (not shown) is Angra dos Reis with almost complete phase separation of

70 Kirschsteinitic olivine from Fo-Fa olivine. Figure 2 illustrates the major element chemistry of
71 angrite olivines from this study. Figure 2a compares CaO (wt.%) vs. MgO (wt.%), while Figure
72 2b examines MnO (wt.%) vs. MgO (wt.%). The arrows point in the direction of increasing
73 fractionation. Note that Ca and Mn are enriched toward the grain rims, right to left, in the NWA
74 10463 olivine (red symbols). However, upon exsolution (the points all the way to the left, Ca
75 increases while Mn decreases. Figure 3 is the new olivine Mn vs. Fe diagram showing Mars,
76 Earth, angrite parent body, and Moon. Figure 3a includes all of the olivine data, including Ca-
77 rich olivines, while Figure 3b only plots olivine with Ca below 5 mol.% on a Ca-Mg-Fe plot. As
78 with pyroxene, the inclusion of Ca in the olivine structure changes the partitioning behavior of
79 Mn relative to Fe. Again, this can be seen in the trend of the exsolution tie-lines in Figure 2. For
80 the purpose of determining planetary parentage, one can still use the Mn/Fe ratio in olivine,
81 provided the olivine does not have a substantial Ca component, hence the 5 mol.% limit.
82 Meteorites LEW 86010 and Angra dos Reis are not plotted here, as they cannot be used
83 effectively on the Mn vs. Fe diagram because they are thermally annealed. Figure 4 illustrates
84 olivine quadrilaterals for five angrite meteorites, unequilibrated angrites SAH 99555, NWA
85 10463, LEW 87051 and equilibrated LEW 86010 and Angra dos Reis. Figure 4 shows that two
86 meteorites plotted on the left reflect olivine-melt partitioning before exsolution (i.e., SAH 99555
87 and LEW 87051), the two on the right only reflect subsolidus partitioning between two olivine
88 solid solutions, while NWA 10463 shows aspects of both. Figure 5 is the revised Fe/Mn vs.
89 anorthite content in plagioclase diagram with the new location for the angrite parent body in
90 close proximity to the Earth and Moon. As opposed to Figure 4 in Papike et al. (2003), this
91 figure plots angrite olivine, avoiding the complications inherent to measuring Fe/Mn ratios in
92 high Ca pyroxenes already discussed above.

93

94

DISCUSSION

95 **The role of crystal chemistry in the efficacy of olivine as a recorder of planetary parentage**

96 The compositions of the Ca-Fe-Mg olivines can be displayed on an olivine quadrilateral
97 (see Fig. 4). There is complete solid solution between monticellite (CaMgSiO_4) and
98 kirschsteinite ($\text{CaFe}^{2+}\text{SiO}_4$) as well as between forsterite (Mg_2SiO_4) and fayalite ($\text{Fe}^{2+}_2\text{SiO}_4$) at
99 high temperatures. However, at low temperatures there is a large miscibility gap between these
100 two solid solutions. Fittipaldo et al. (2005) studied the thermal histories of Angra dos Reis and
101 LEW 86010. These authors also estimated the dependence of the olivine solvus between high
102 and low Ca olivines as a function of both composition and temperature. Olivine-kirschsteinite
103 pairs in Angra dos Reis record a closure temperature of 600-650 °C, while LEW 86010 has an
104 estimated closure temperature of 700-720 °C. The meteorites studied here have variable cooling
105 histories with SAH 99555 cooling the fastest, therefore representing a good approximation of a
106 melt composition. Second in estimated cooling rate is NWA 10463, with exsolution in olivine
107 only in the Fe-rich rims. Third is LEW 86010 with well developed exsolution in olivine in two
108 directions. Slowest in cooling rate is Angra dos Reis with phase separation of the high-Ca and
109 low-Ca olivines (see Fig. 2a). The M2 site is more compliant than the M1 site and can become 8-
110 coordinated and accommodate Ca. The M1 site is smaller and remains octahedral. Figure 2 tells
111 much of the important site occupancy story. Note that Ca and Mn follow a similar trend (core to
112 rim) with both increasing toward the rim (SAH 99555 and NWA 10463) until the onset of
113 exsolution. This represents a normal igneous zoning trend for two relatively incompatible
114 elements, with Ca being the more incompatible as evidenced by the slopes on the plot. However
115 with exsolution (meteorites LEW 86010 and Angra dos Reis, and to a lesser extent NWA 10463)

116 Mn and Ca go into separate phases, with Ca in the exsolved kirschsteinitic olivine, and Mn
117 retained in the Fo-Fa olivine. Manganese goes into the M2 site of low-Ca olivine.

118 Papike (1981) recognized that in any one planetary body there were a number of Mn/Fe
119 slopes for different basaltic environments. For example for Earth, seven different environments
120 were compared and differences were noted (Papike, 1981). Also for the moon, significant
121 differences were observed between high- and low- Ti basalts (Papike et al., 1976). The Fe/Mn
122 ratio of a given mineral phase in a planetary body results from several different factors, but can
123 be broadly categorized into differences in the initial bulk silicate composition or differences
124 resulting from changes to the partitioning behavior of Fe relative to Mn. With respect to the
125 former, the initial Fe/Mn ratio results from the initial bulk composition of a planetary body and
126 early processes which may alter this ratio such as differentiation and core formation. For
127 example, sequestering metallic Fe into a planetary core will lower the initial Fe/Mn of its
128 derivative mantle. On the other hand, changes in the partitioning behavior of Fe relative to Mn
129 can result from differences in bulk melt chemistry (NBO/T), or differences in mineral
130 chemistries Mn (i.e., “QUAD” pyroxene vs. fassaite, Al, Ti-rich calcic- pyroxene). Finally
131 dynamic changes in the fO_2 of the crystallizing melt can also significantly alter the crystal/melt
132 partitioning behavior of Fe. When we refer to the partitioning behavior of Fe vs. Mn into a
133 silicate phase, whether it is olivine or pyroxene, we are really referring to the partitioning of Fe^{2+}
134 vs. Mn^{2+} . Consider two olivines crystallizing from equivalent melts (same chemistry and bulk
135 Fe/Mn), different only in the fO_2 of crystallization, one may measure different Fe/Mn ratios. In
136 the more oxidizing environment, the Fe^{3+}/Fe^{Total} in the liquid will be higher, resulting in a lower
137 apparent Fe/Mn in the olivine, as the compatibility of $Fe^{3+} \ll Fe^{2+}$. This is not likely a concern
138 with the angrites presented in this study. The inclusion of Fe^{3+} in the olivine structure requires a

139 coupled substitution, for example, Al^{3+} in the tetrahedral site, for Si^{4+} . The molar
140 concentration of Al^{3+} in olivine can therefore be seen as an upper limit to the Fe^{3+} concentration,
141 and a quick look at the electronic appendices for all of the angrite olivines demonstrates that Al,
142 and hence Fe^{3+} , is very limited. All of these factors can affect Fe/Mn trends for a given mineral
143 phase in a planetary body. This explains the spread observed in the planetary trends for olivine
144 and pyroxene in Papike et al. (2003). Despite this, the fact remains that each planetary body has a
145 distinct, over-arching trend that is the fingerprint of the planetary source or planetary parentage.
146 This paper improves the “tool” for planetary parentage. It does not explain why it works, the
147 planetary dispersion of Mn/Fe ratio, or the apparent correlation between Mn/Fe slope and
148 heliocentric distance.

149 **Intra- and Inter- planetary differences in Mn-Fe systematics**

150 In a book by Stuart Ross Taylor “Solar System Evolution,” Taylor (1992) discusses the
151 systematic differences in planets with heliocentric distance from the Sun. One noteworthy
152 observation was increasing iron-rich core size with increasing proximity to the Sun. Taylor also
153 notes the increased volatile element concentration in planets with increasing distance from the
154 Sun. With respect to Mn, one would expect the bulk silicate Mn/Fe ratio of a planet to increase
155 with increasing heliocentric distance because Mn is more volatile than iron and would be lost
156 relative to iron near the Sun. Core formation serves to sequester Fe into a planet’s core, so that
157 one would expect planets with larger cores (i.e., those closer to the Sun) to have proportionally
158 less Fe in their silicate mantles than those with smaller cores. The cumulative effects suggest that
159 the silicate mantles of planets closer to the Sun should have both less Mn and Fe than those
160 further from the Sun. Perhaps it is somewhat surprising, then, that the Mn/Fe ratios still seem to
161 show an overarching correlation with heliocentric distance (Fig. 1, Papike et al. 2003; Fig. 3, this

162 paper). We believe that the Earth, Moon, and Angrite Parent Body (APB) came from a similar
163 planetary reservoir.

164

165

IMPLICATIONS

166 Many of our past studies have explored how the chemical systematics of important rock-
167 forming minerals including pyroxene, olivine and feldspar, can provide important clues to their
168 planetary parentage and subsequent thermal and oxygen fugacity histories. The major
169 implications of the present study indicate is that a very important solar system reservoir for the
170 angrite meteorites is very similar to the terrestrial solar system reservoir. The major difference
171 between angrite basaltic melts and terrestrial basaltic melts is the severe volatile and alkali
172 element depletion leading to the presence of almost pure anorthite plagioclase in angrite basalts.
173 We suggest that one way of getting this volatile depletion is that an asteroid sized parent body
174 for angrites condensed from a hot vapor cloud, resulting in volatile depletion. Keil (2012), in his
175 excellent review of angrites, discusses this topic and concludes that the angrite parent body
176 (APB) must have been >100 km in radius. Keil (2012) also points out that some angrites, for
177 example D'Orbigny, contain vesicles indicating vapor lost and suggested the vapor is dominated
178 by CO₂. He also observes that angrites do not contain obvious features of a shock or brecciation
179 history. Our earlier paper (Papike et al. 2003) indicated that the Mn/Fe slope might suggest that
180 the location of the angrite parent body was close to the Sun and perhaps might even be Mercury.
181 We think many more recent studies can rule out Mercury as the source.

182 We are not suggesting that angrites are early Solar System condensates (e.g., CAIs).
183 Their parent body may reflect condensation but they are true basalts that experienced melt
184 evolution. The accreting material was likely CI chondrites, as for Earth. In summary, this paper

185 improves an important tool for determining planetary parentage. It is observed, but not yet
186 completely understood, that the mantle source that gave rise to planetary basalts on the bodies 4
187 Vesta, Mars, Earth, angrite parent body, and Moon have differing Mn/Fe slopes that show a
188 correlation with heliocentric distance with the exception for APB and Moon which may show
189 signs of volatile loss of Mn. Volatility of Mn and core formation both affect the Mn/Fe ratio in
190 planetary basalts. Despite this, each planetary body is characterized by a unique trend.

191

192

ACKNOWLEDGEMENTS

193 We gratefully acknowledge NASA funding to C. Shearer, and Alison Santos for her
194 analytical work on NWA 10463.

195

196

REFERENCES CITED

197 BVSP (Basaltic volcanism study project) (1981) Basaltic volcanism on the terrestrial planets.

198 Pergamon, New York, 1286 p.

199 Fittipaldo, M.M., Jones, R.H., and Shearer, C.K. (2005) Thermal histories of angrite meteorites:

200 Trace element partitioning among silicate minerals in Angra dos Reis, Lewis Cliff 86010,
201 and experimental analogs. *Meteoritics & Planetary Science*, 40, 573-589.

202 Keil, K. (2012) Angrites, a small but diverse suite of ancient, silica – undersaturated volcanic-
203 plutonic mafic meteorites, and the history of their parent asteroid. *Chemie der Erde*, 72,
204 191-218.

205 Papike, J.J. (1981) Silicate mineralogy of planetary basalts, in *Basaltic Volcanism on the*
206 *Terrestrial Planets*. Lunar and Planetary Institute, Houston, Texas, 340-363.

- 207 Papike, J.J., Hodges, F.N., Bence, A.E., Cameron, M., and Rhodes, J.M. (1976) Mare basalts:
208 crystal chemistry, mineralogy, and petrology. *Review of Geophysics*, 14, 475-540.
- 209 Papike, J.J., Karner, J.M., and Shearer, C.K. (2003) Determination of planetary basalt parentage:
210 a simple technique using the electron microprobe. *American Mineralogist* 88, 469-472.
- 211 Papike, J.J., Burger P.V., Bell A.S., and Shearer C.K. (2016a) Angrite olivine as a Solar System
212 recorder of $^{53}\text{Mn} - ^{53}\text{Cr}$ chronology of their early crystallization: Implications of olivine
213 crystal chemistry and subsolidus reactions for the partitioning of Cr and Mn and the re-
214 setting of the Mn-Cr chronometer. In *Lunar and Planetary Science* 47, Abstract no.1752,
215 Lunar and Planetary Science Institute, Houston.
- 216 Taylor, S.R. (1992) *Solar system evolution: A new perspective*. Cambridge University Press,
217 Cambridge. 307 p.

218 **FIGURE CAPTIONS**

- 219 Figure 1. BSE, Mg, Ca, Mn, Cr maps of SAH 99555, NWA 10463, and LEW 86010. This is also
220 the cooling sequence, with SAH 99555 representing a melt composition and showing primary
221 growth zoning which enables the $^{53}\text{Mn}-^{53}\text{Cr}$ chronometer. NWA 10463 represents the next step
222 in cooling history with exsolution lamellae appearing in the Fe-rich outer zones of olivine. LEW
223 86010 has well developed exsolution throughout the olivine grains. Phases are labeled as
224 follows: ol = olivine, pyx = pyroxene, an = anorthite. Bright white areas in the NWA 10463 Ca
225 map are thought to be terrestrial alteration (carbonate?), but have not been identified.
- 226 Figure 2. Major element chemistry of angrite olivines from this study. (a) CaO (wt.%) vs. MgO
227 (wt.%). (b) MnO (wt.%) vs. MgO (wt.%). Tie lines connect the exsolved olivine phases.
- 228 Figure 3. Mn vs. Fe systematics for angrite olivine for 5 angrite meteorites. (a) All angrite
229 olivine analyses meeting stoichiometric requirements. (b) Angrite olivine analyses meeting

230 stoichiometric requirements and with <5 mol.% of the Ca-olivine end member. The asterisk here,
231 and in Fig. 5, is used to denote this subset of angrite olivines. These are the olivines that should
232 be used to determine the Mn/Fe ratio.

233 Figure 4. Olivine quadrilaterals for 5 angrite meteorites, unequilibrated SAH 99555, NWA
234 10463, LEW 87051 and equilibrated LEW 86010 and Angra dos Reis. Olivine endmembers
235 include forsterite (Fo; Mg_2SiO_4), fayalite (Fa; Fe_2SiO_4) monticellite (Mo; $CaMgSiO_4$) and
236 kirschsteinite (Ki; $CaFeSiO_4$). The trends represent well documented fractionation trends of
237 olivine crystallizing from melt followed by exsolution near the Fe-rich portion of the QUAD.

238 Figure 5. Diagram plotting Fe/Mn ratio in angrite pyroxene and olivine (X-axis) vs. anorthite
239 content of angrite plagioclase (Y-axis). The asterisk here indicates only those angrite olivines
240 with <5 mol.% of the Ca-olivine end member were used to define the angrite field. This diagram
241 was revised after Papike et al. (2003; Fig. 4), and was constructed using the same methodology.
242 The solid vs. hashed outlines serve to distinguish pyroxene from olivine, respectively.

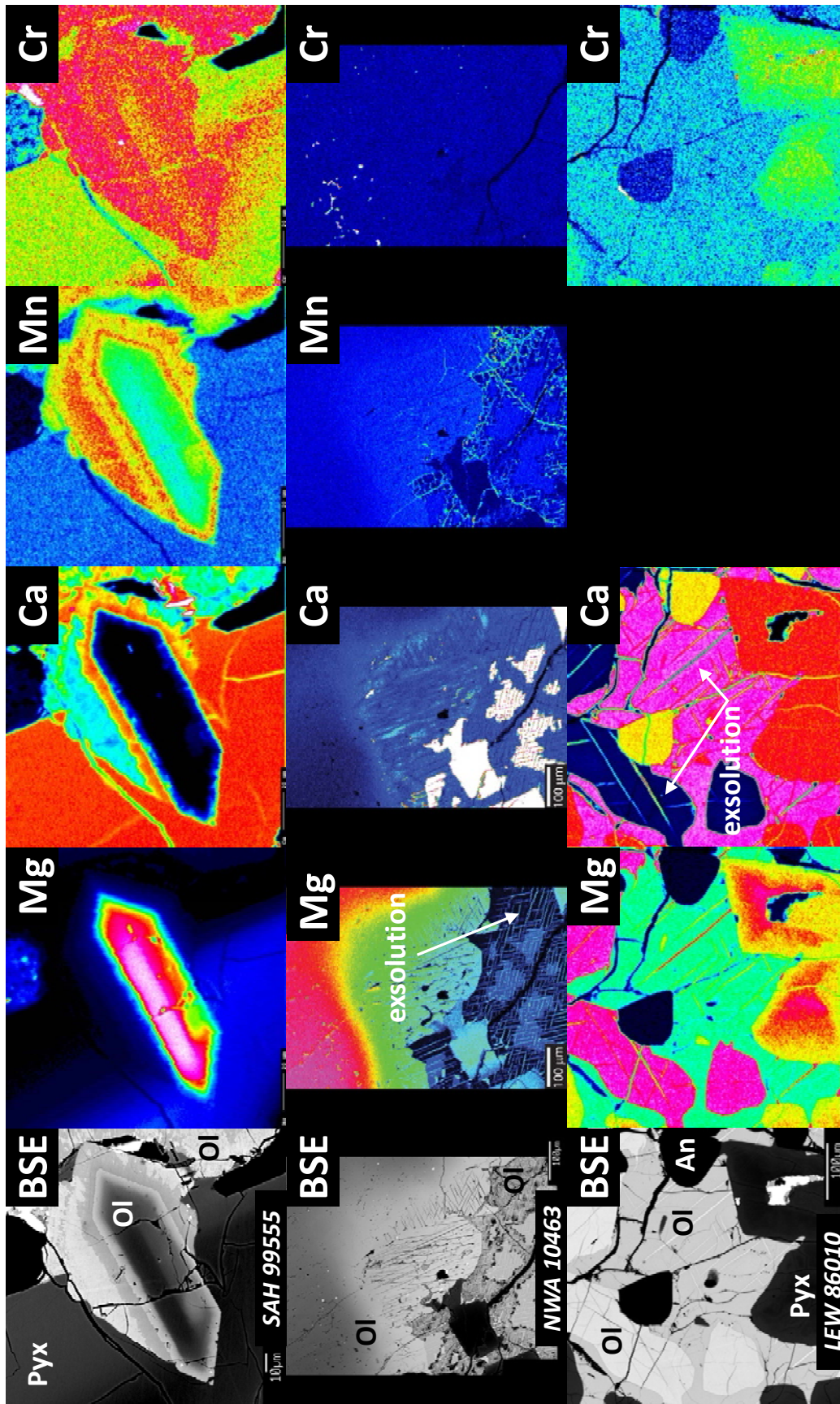


Figure 1.

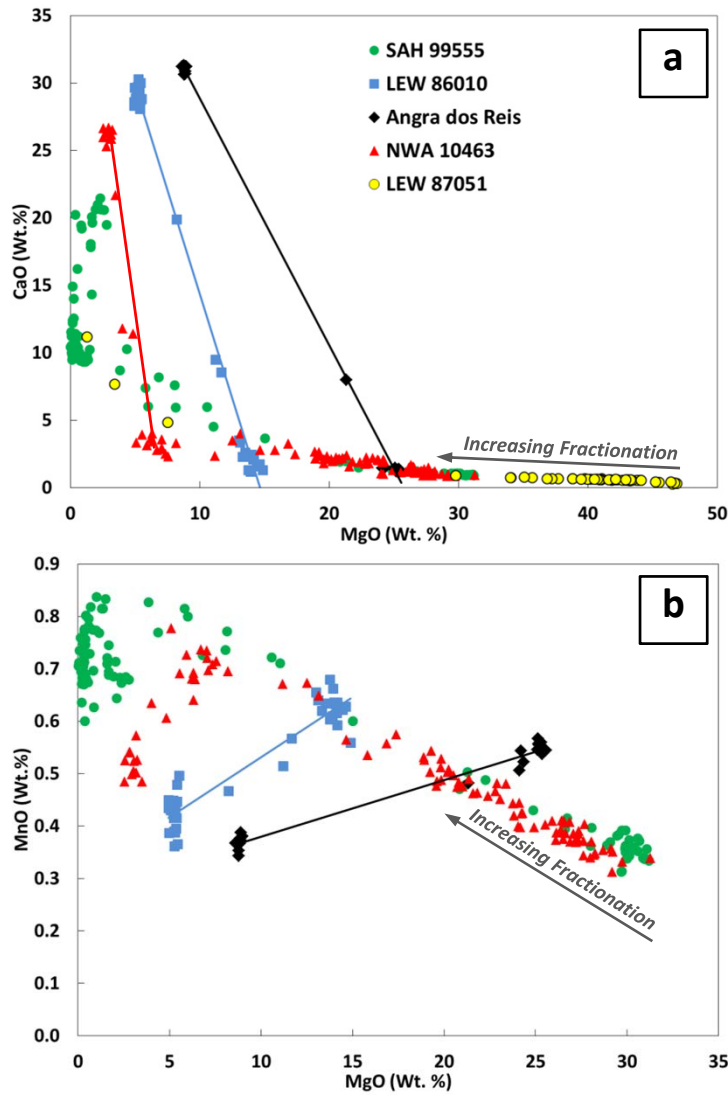


Figure 2.

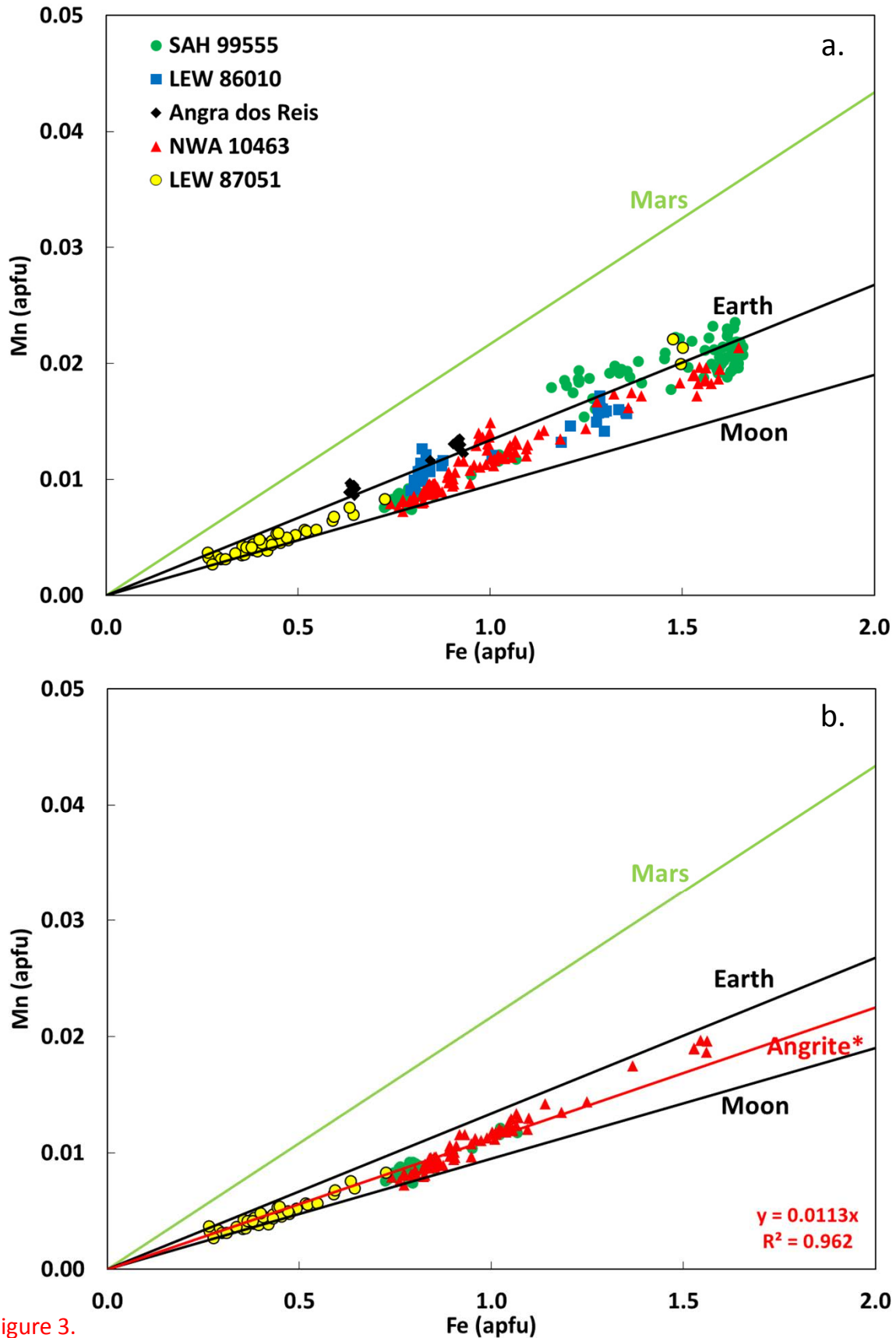


Figure 3.

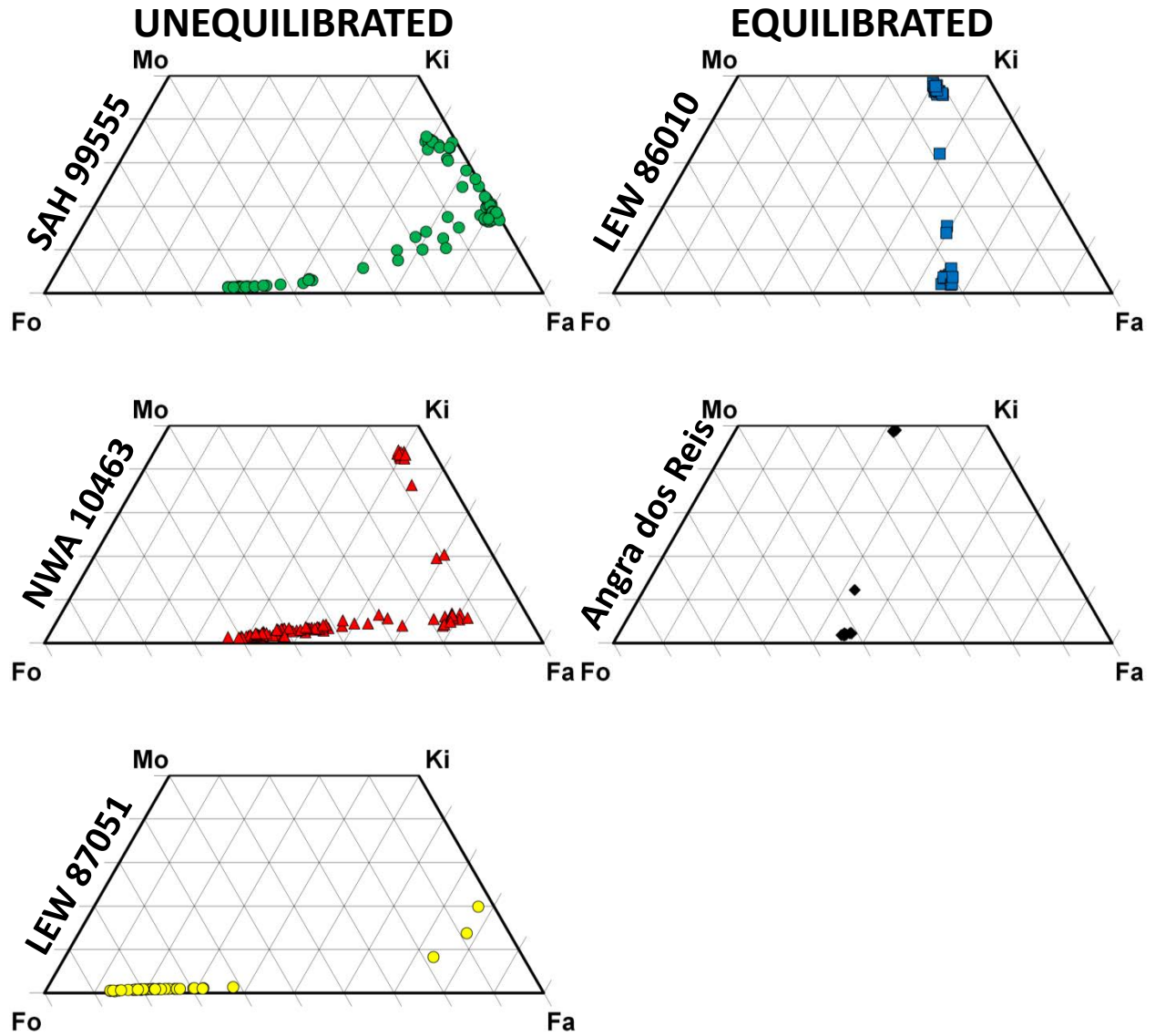


Figure 4.

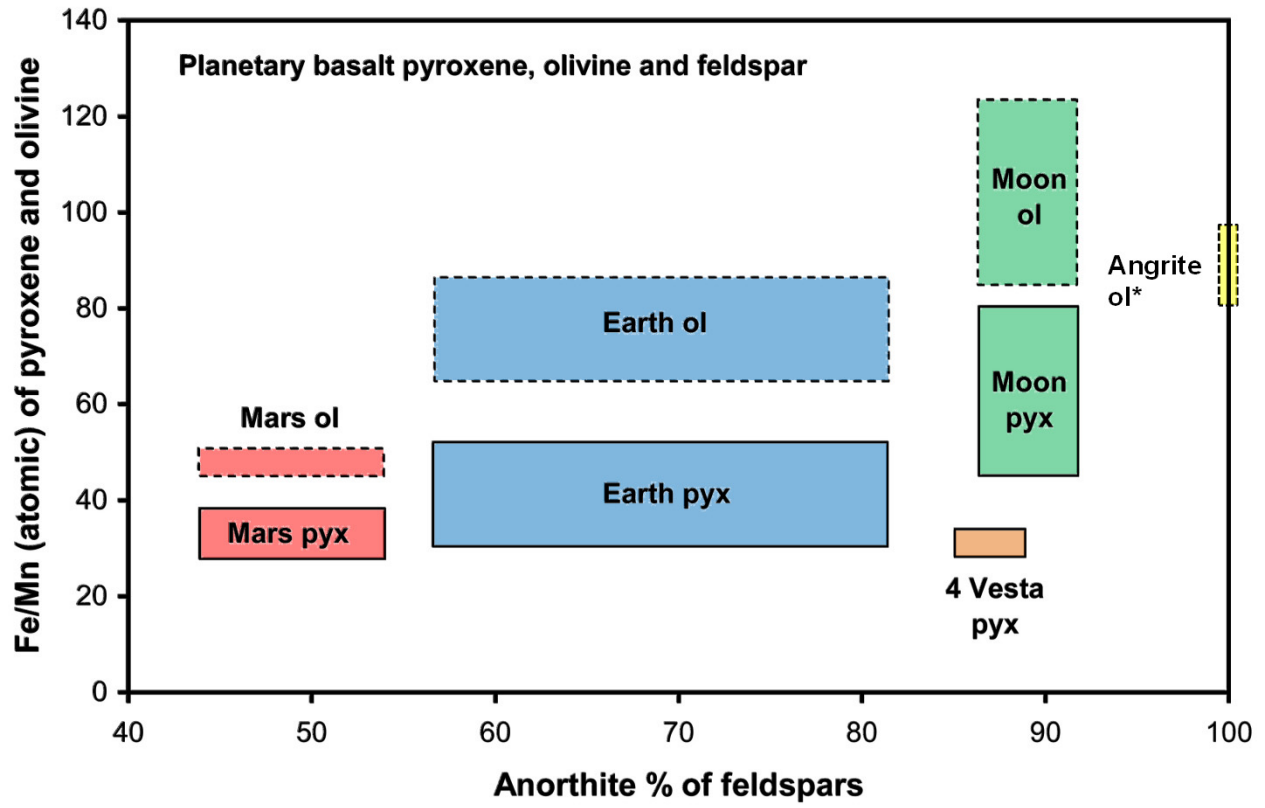


Figure 5.